

## Controlled Shock Shells and Intracluster Fusion Reactions in the Coulomb Explosion of Very Large Clusters

F. Peano<sup>1</sup>, R.A. Fonseca<sup>2</sup>, M. Marti<sup>2</sup>, S. Martins<sup>2</sup>, J.L. Martins<sup>2</sup>, L.O. Silva<sup>2</sup>

<sup>1</sup> *Dipartimento di Energetica, Politecnico di Torino, Italy*

<sup>2</sup> *GoLP/Centro de Física dos Plasmas, Instituto Superior Técnico, Lisboa, Portugal*

**Abstract.** The ion dynamics in the Coulomb explosion of very large ( $\sim 10^6 - 10^7$  atoms) deuterium clusters irradiated by two subsequent laser pulses having different intensities is analyzed using an approximate one-dimensional theory, where a prescribed electron dynamics, related to the pulse envelope, is assumed. Suitable sets of pulse intensities and delays between the pulses may drive the formation of large-scale shock shells, thus leading to intracluster fusion reactions. The validity of the results is confirmed with highly-realistic, three-dimensional particle-in-cell simulations.

### 1. INTRODUCTION

Large deuterium (D) clusters ( $\sim 10^6 - 10^7$  atoms) irradiated by ultra-short (tens of fs) and ultra-intense ( $I \sim 10^{18} - 10^{22}$  W/cm<sup>2</sup>) laser pulses explode producing highly-energetic D ions ( $E \sim 100$  keV), capable of driving nuclear fusion reactions [1]. Among the various physical scenarios arising from the laser-cluster interaction, the formation of multiple-velocity structures in the ion phase-space, called shock shells [2], is of great interest, as it can lead to energetic collisions within single exploding clusters. While small-scale structures may form spontaneously during the Coulomb explosion of large clusters hit by a single laser pulse [3], large-scale, pronounced shock shells can be easily obtained, and controlled, using two sequential pulses (e.g. a weak pulse followed by an ultra-intense one, with a proper time delay  $\Delta t$ ) [3]. The ability of generating large-scale shock shells and tailoring the ion phase-space dynamics opens the way to intracluster fusion reactions. Such reactions constitute a novel, different phenomenon with respect to the intercluster reactions observed so far. In particular, the intracluster reaction rate exhibits a sharp, narrow peak ( $\sim 10 - 50$  fs wide) immediately after the shock formation. As for very large clusters (initial radius  $\sim 100$  nm), the intracluster and intercluster fusion yields are comparable, an ideal double-pump experiment should furnish a clear evidence for the occurrence of intracluster, shock-driven fusion reactions.

### 2. ONE-DIMENSIONAL MODEL FOR THE COULOMB EXPLOSION

A proper tuning of the double-pump parameters requires a deep knowledge of their influence on the explosion dynamics, the shock shell formation and evolution, and, consequently, the intra-cluster fusion yield. As a direct parameter scan via complete numerical simulations of the laser-cluster interaction would have been too computationally demanding, we developed a simple one-dimensional (1D) theoretical model that allowed us to

investigate the effects of the principal double-pump parameters, namely the time delay between the pulses,  $\Delta t$ , and the peak intensity of the first pulse,  $I_1$ .

Our model is an extended version of the standard model for the Coulomb explosion of a spherical pure-ion cluster (cf. [2]), which takes into account the neutralizing effect of the electron population in the expanding cluster with a prescribed dynamics, determined uniquely by the laser pulse features. In these framework, the acceleration of an ion at a given time  $\tau$  and radial position  $r$  is written, in dimensionless units, as

$$\frac{d^2 r}{d\tau^2} = \frac{Q(r) - Q_{el}(r, \tau)}{r^2} \quad (1)$$

where we normalize mass to  $m$  (ion mass), length to  $R_0$  (initial cluster radius), charge to the elementary charge  $e$ , and time to  $t_0 = \sqrt{(mR_0^3)/(e^2 N_0)}$ , being  $N_0$  the total number of ions. The quantity  $Q(r)$  is the ion charge within a sphere of radius  $r$ , while  $Q_{el}(r, \tau)$  describes the absolute value of the electron charge still present within the same sphere at time  $\tau$ . The latter is then related to the instantaneous value of the laser envelope function,  $E_1(\tau)$ , by  $E_1(\tau)/\sqrt{2} = [1 - Q_{el}(r, \tau)]/R^2$ , where  $R$  is the cluster radius at time  $\tau$  and the  $\sqrt{2}$  factor accounts for the periodicity of the laser electric field [4]. At each time  $\tau$ , the electrons remaining within the cluster are assumed to fully neutralize the cluster core, so that only the ions having radius greater than that of the electron distribution,  $R_{el}(\tau)$ , are allowed to move.

The validity of the results has been confirmed with highly-realistic, three-dimensional (3D), particle-in-cell (PIC) simulations in the OSIRIS framework [5], treating self-consistently the 3D dynamics of electrons and ions in the laser field, the outer ionization dynamics, and the full dynamics of both the slow expansion induced by the first pulse and the sudden explosion driven by the second pulse.

### 3. INTRACLUSTER FUSION REACTIONS

Large-scale shock shells are characterized by a well-defined multi-branch structure in phase space, most frequently a three-branch structure like the ones in Fig. 3. As the explosion goes on, the upper branch overlaps the lower branches: the shock shell widens radially, narrowing its velocity spread, and, meanwhile, the ion density on each branch decreases. Therefore, one can reasonably expect the probability of nuclear reactions between ions belonging to different branches to be higher in the early stages after the shock shell formation and to decrease rapidly at advanced times. From the solution of Eq. (1), the intracluster reaction rate,  $\mathbf{R}$ ; and the total number of reaction per cluster,  $N_r$ , are readily evaluated by

summing up all the contributions arising from collisions among ions on different velocity branches. By doing so, one can investigate the influence of  $I_1$  and  $\Delta t$  on  $N_r$ , seeking the combination of parameters that maximizes it.

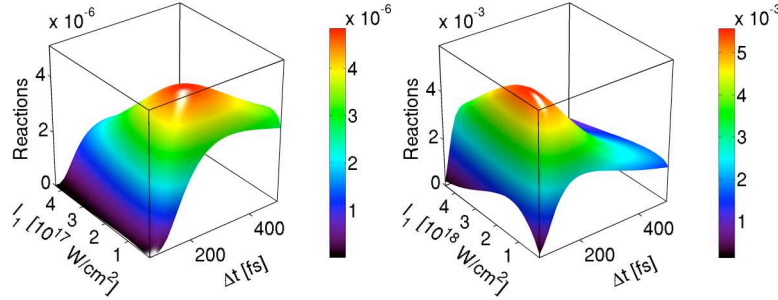


FIG. 1: Number of reaction per cluster,  $N_r$ , vs.  $I_1$  and  $\Delta t$ , for  $R_0 = 32$  nm (left) and  $R_0 = 100$  nm (right).

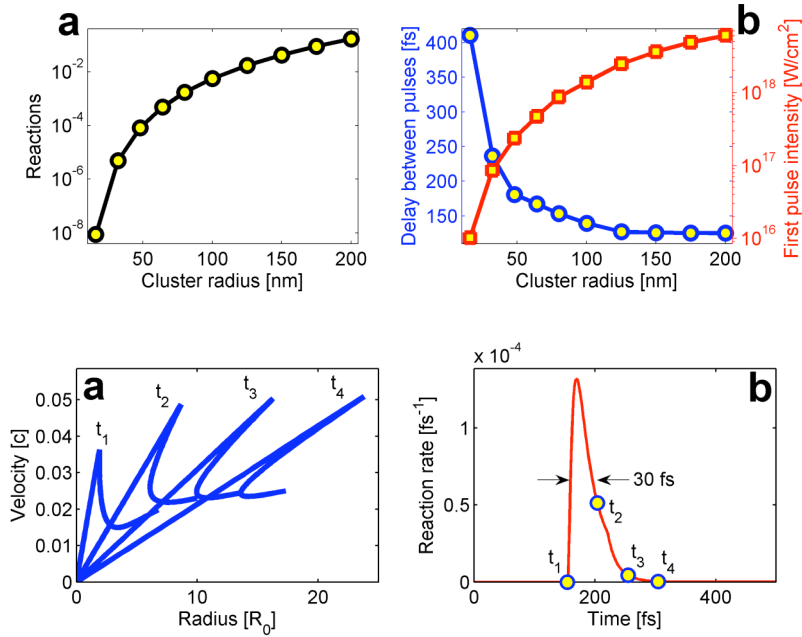


FIG. 2: Peak value of  $N_r$  (a), and optimal value of  $I_1$  (red) and  $\Delta t$  (blue) (b), for different values of  $R_0$ . FIG. 3: Phase space profile at times  $t_1 = 155$  fs,  $t_2 = 205$  fs,  $t_3 = 255$  fs,  $t_4 = 305$  fs (a) and history of the reaction rate,  $R$  (b), for  $R_0 = 100$  nm, and with the optimal double pump parameters:  $I_1 = 1.4 \cdot 10^{18}$  W/cm<sup>2</sup> and  $\Delta t = 139$  fs.

Here, we present results from parametric studies, with respect to  $I_1$  and  $\Delta t$ , for several cluster sizes, with initial radii,  $R_0$ , in the range 16-200 nm. For each  $R_0$ , we consider a spherical D cluster (with uniform atomic density,  $n_0 = 4.56 \cdot 10^{22}$  cm<sup>-3</sup>) hit by a pulse sequence in which a weak laser pulse (peak intensity  $I_1$  (variable), central wavelength  $\lambda_0 = 820$  nm, duration  $\sim 35$  fs) is followed by an ultra-intense pulse (peak intensity  $I_2 \gg I_1$ , central wavelength  $\lambda_0 = 820$  nm, duration  $\sim 20$  fs) with time delay  $\Delta t$  variable in the range 70-500 fs. Figure 1 shows  $N_r$  as a function of  $I_1$  and  $\Delta t$ , for two representative cases:  $R_0 = 32$  nm (FIG a) and  $R_0 = 100$  nm (FIG b). With  $R_0 = 32$  nm,  $N_r$  assumes its maximum value,  $N_r^* = 4.85 \cdot 10^{-6}$  reactions, for  $I_1 = 8.6 \cdot 10^{16}$  W/cm<sup>2</sup> and  $\Delta t = 236$  fs, while, with  $R_0 = 100$  nm,  $N_r^* = 5.58 \cdot 10^{-3}$  reactions for  $I_1 = 1.4 \cdot 10^{18}$  W/cm<sup>2</sup> and  $\Delta t = 139$  fs. The dependence of the optimal combination

of  $I_1$  and  $\Delta t$  on the initial cluster size is depicted in Fig. 2, along with the correspondent variation of  $N_r^*$ , while Fig. 3 shows the time history of the phase space profile and the evolution of  $N_r$ , for  $R_0 = 100$  nm in the optimal case. Figure 4 reports a comparison between the intracluster fusion yield,  $Y_{ic}$ , and the intercluster fusion yield,  $Y_{IC}$ , for different values of  $R_0$ . The comparison has been carried out by assuming a fixed, cylindrical reaction volume containing a given number of D ions (fixed as well). For the evaluation of  $Y_{IC}$ , the simple formula  $Y_{IC} = \bar{n}^2 \langle \sigma v \rangle V_r T_d$  has been used, where  $\bar{n} = 10^{19} \text{ cm}^{-3}$  is the average ion density the reaction volume  $V_r$  is that of a cylinder with radius  $R_r = 100 \mu\text{m}$  and height  $H_r = 2 \text{ mm}$ ,  $T_d = \pi R_r / (2v_{\text{max}})$  is the plasma disassembly time ( $v_{\text{max}}$  being the maximum ion velocity), and  $\langle \sigma v \rangle$  has been evaluated using the asymptotic energy spectra obtained from Eq. (1).

Finally, Fig. 5 shows a comparison between the ion dynamics predicted by Eq. (1) and that obtained with a 3D PIC simulation, for the optimal case of Fig. 1a. (in the simulation,  $I_1$  has been lowered to  $I_1 = 2 \cdot 10^{16} \text{ W/cm}^2$  to compensate for hydrodynamics effects).

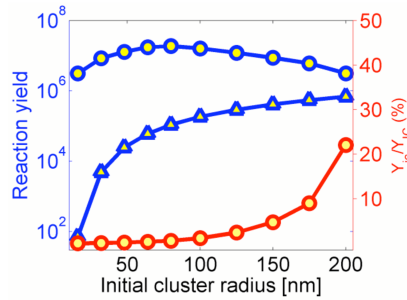


FIG. 4: Intercluster fusion yield,  $Y_{IC}$  (blue circles), intracluster fusion yield,  $Y_{ic}$  (blue triangles), and percentage value of  $Y_{ic}/Y_{IC}$  (red), for different values of  $R_0$ .

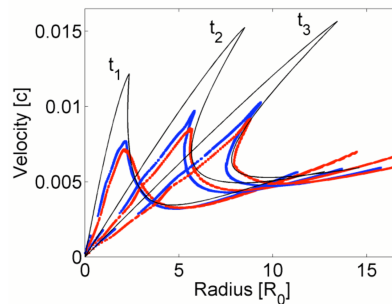


FIG. 5: Phase space profile at times  $t_1 = 270$  fs,  $t_2 = 315$  fs,  $t_3 = 350$  fs. Colored points mark the position in the phase space for those particles contained in a solid angle  $\Delta\Omega \sim 0.1$  sr around the polarization (red) and transverse (blue) directions. Thin black lines refer to the solution of Eq. (1).

## REFERENCES

- [1] T. Ditmire *et al.*, Nature **386**, 54 (1997); T. Ditmire *et al.*, Nature **398**, 489 (1999).
- [2] A.E. Kaplan *et al.*, Phys. Rev. Lett. **91**, 143401 (2003).
- [3] F. Peano, *et al.*, Phys. Rev. Lett. **94**, 033401 (2005).
- [4] I. Last and J. Jortner, J. Chem. Phys. **120**, 1336 (2004).
- [5] R.G. Hemker, UCLA PhD Thesis (2000); R.A. Fonseca *et al.*, Lect. Notes Comp. Sci. **2329**, III-342 (Springer-Verlag, Heidelberg, 2002).